HAL
open science

Fusing ground measurements and satellite-derived products for the construction of climatological maps in atmosphere optics

Mireille Lefèvre, Jan Remund, Michel Albuisson, Thierry Ranchin, Lucien Wald

To cite this version:

Mireille Lefèvre, Jan Remund, Michel Albuisson, Thierry Ranchin, Lucien Wald. Fusing ground measurements and satellite-derived products for the construction of climatological maps in atmosphere optics. 23rd EARSeL Annual Symposium "Remote Sensing in Transition", Jun 2003, Ghent, Belgium. pp.85-91. hal-00395054

HAL Id: hal-00395054
https://hal.science/hal-00395054v1

Submitted on 14 Jun 2009

HAL is a multi-disciplinary open access archive for the deposit and dissemination of scientific research documents, whether they are published or not. The documents may come from teaching and research institutions in France or abroad, or from public or private research centers.

L'archive ouverte pluridisciplinaire **HAL**, est destinée au dépôt et à la diffusion de documents scientifiques de niveau recherche, publiés ou non, émanant des établissements d'enseignement et de recherche français ou étrangers, des laboratoires publics ou privés.

Fusing ground measurements and satellite-derived products for the construction of climatological maps in atmosphere optics

M. Lefèvre
Groupe Télédétection et Modélisation, Ecole des Mines de Paris, B.P. 207 - 06904 Sophia Antipolis cedex, France

J. Remund
METEOTEST, Fabrikstrasse 14, 3012 Bern, Switzerland

M. Albuisson, T. Ranchin & L. Wald
Groupe Télédétection et Modélisation, Ecole des Mines de Paris, B.P. 207 - 06904 Sophia Antipolis cedex, France

Keywords: data fusion, solar radiation, Linke turbidity factor, remote sensing, resampling

ABSTRACT: Climatological maps (gridded data) of optical parameters of the atmosphere often result from application of numerical models or processing of satellite images. Such maps usually exhibit very large cell sizes, of the order of 1° of arc angle. There is a need to increase their spatial resolution to obtain a cell size closer to the spatial representation obtained by standard meteorological instruments at ground level, i.e. 5' of arc angle. It then permits to fuse ground measurements and gridded data, especially to correct for bias observed in gridded data. Taking advantage of the availability of other data sets of relevance to the parameter under concern, though different, a method is proposed for the synthesis of the initial gridded data at a higher resolution by the means of a fusion process. This paper describes the method with an application for the construction of worldwide maps of the Linke turbidity factor with cells of 5' in size. This factor characterises the atmospheric optical turbidity under clear skies and is a very important parameter in solar radiation studies.

1 INTRODUCTION

Gridded data in environment often result from application of numerical models (e.g., weather models) or processing of satellite images. Examples are climatological maps of geophysical parameters, e.g., air temperature or ozone content. Such maps usually exhibit very large cell sizes, of order of 1° of arc angle. There is a need to increase their spatial resolution for further processing. One example is the need to obtain a cell size close to the spatial representation obtained by standard meteorological instruments at ground level, i.e. 5' of arc angle. It then permits to fuse ground measurements and gridded data, especially to correct for bias observed in gridded data (Beyer *et al.* 1997; D'Agostino & Zelenka 1992).

The problem is that such climatological maps only exist at low spatial resolution. A resampling of the maps at a finer cell size does not actually increases the spatial resolution of the data since no additional knowledge is brought. Taking advantage of the availability of other data sets of relevance to the parameter under concern, though different, a method is proposed for the synthesis of the initial gridded data at a higher resolution by the means of a fusion process.

2 PROBLEM STATEMENT

Be a set of gridded data $S(0)_{r0}$ available at a spatial resolution *r0* (taken here as equivalent to the cell size). $S(0)$ may be multi-modality. Let be other sets of gridded data $S(i)_{ri}$, i=1..N, exhibiting spatial resolution *ri*. The sets $S(i)$ are ranked by decreasing cell sizes, *rN* is the smallest cell size (the highest spatial resolution). The sets $S(i)$ can be multi-modality.

It is assumed that $S(i)$ and $S(0)$ are geometrically aligned. It is further assumed that each $S(i)_r$ can be associated to $S(0)_r$, that is a relation exists between these data sets for a given resolution *r*.

The problem is the synthesis of $S(0)_{rN}$.

3 THE ARSIS CONCEPT AND THE GENERAL SOLUTION

The application of the ARSIS concept is one solution to this problem. The acronym ARSIS stands for the French "Amélioration de la Résolution Spatiale par Injection de Structures", which means “spatial resolution enhancement by injection of structures” (Ranchin *et al.* 2003; Ranchin & Wald 2000; Wald 2002).

Under this concept, it is considered that the missing knowledge permitting to synthesize $S(0)_{RN}$ from $S(0)_{r0}$, is composed of the spatial high-frequencies (formally, wavevectors) of $S(0)$ comprised between [1/(2 r0), 1/(2 rN)]. This range of high frequencies

(noted HF) is present in the other data sets, e.g., S(i) exhibits frequencies in [1/(2 r0), 1/(2 ri)]. An appropriate modeling permits to synthesize the searched $S(0)HF$ from the known $S(\mathrm{i})HF$. Then the application of a multi-scale model (MSM) constructs $S(0)_{rN}$, starting from $S(0)_{r0}$ and using the estimated HF.

4 ASSESSING S(0)HF

$S(0)_{r0}$ does not exhibit frequencies greater than 1/(2 r0):

$$S(0)HF_r = 0, \text{ for } r < r0 \quad (1)$$

Let note the multi-scale analysis process MSM. The couple of information ($S(\mathrm{i})_{r0}$, $S(\mathrm{i})HF_{r0\text{-}ri}$) made of the approximation of S(i) at resolution *r0* and of the high frequencies of S(i) in [1/(2 r0), 1/(2 ri)] is obtained by applying the MSM to the data set $S(\mathrm{i})_{ri}$:

$$(S(\mathrm{i})_{r0}, S(\mathrm{i})HF_{r0\text{-}ri}) = \mathrm{MSM}(S(\mathrm{i})_{ri}) \quad (2)$$

The MSM process may be the multi-resolution analysis algorithm of Mallat (1989) or Dutilleux (Dutilleux 1989; Starck & Murtagh 1994) or the generalized Laplacian pyramid (Aiazzi *et al.* 1999). The MSM process is invertible and the synthesis process is noted MSM^{-1}

$$S(\mathrm{i})_{ri} = \mathrm{MSM}^{-1}(S(\mathrm{i})_{r0}, S(\mathrm{i})HF_{r0\text{-}ri}) \quad (3)$$

Assume that:

$$S(0)_{r0} = F_0(S(\mathrm{i})_{r0}) + \varepsilon_0 \quad (4)$$

where F_0 and ε_0 are known, e.g., by statistical regression. Note *var*(0) the fraction of variance in $S(0)_{r0}$ explained by $F_0(S(\mathrm{i})_{r0})$. If we write

$$S(0)_{r1}^* = \mathrm{MSM}^{-1}[S(0)_{r0}, var(0)\, F_0(S(\mathrm{i})HF_{r0\text{-}r1})] \quad (5)$$

where $S(\mathrm{i})HF_{r0\text{-}r1}$ is obtained by applying MSM to $S(\mathrm{i})_{ri}$, $S(0)_{r1}^*$ is an estimation of $S(0)_{r1}$.

Because the model F_0 is not exact and was assessed at another resolution *r0* while applied to the interval [r1, r0],

$$(S(0)_{r0}^*, S(0)HF^*_{r0\text{-}r1}) = \mathrm{MSM}(S(0)_{r1}^*) \quad (6)$$

$S(0)_{r0}^*$ is not equal to $S(0)_{r0}$. It should be because the fused product should be identical to the initial product at resolution *r0*. One corrects for it by writing:

$$S(0)_{r1} = \mathrm{MSM}^{-1}(S(0)_{r0}, S(0)HF^*_{r0\text{-}r1}) \quad (7)$$

The process is iterated. At each step and resolution *ri*, are used the sources of data S(i) having a better resolution than *ri*.

At the end of the process, $S(0)_{rN}$ is obtained that is an approximation of the true but unknown gridded data. In any case, this set better represents the reality than what can be obtained by a resampling of $S(0)_{r0}$.

5 APPLICATION CASE

The Linke turbidity factor (TL, for an air mass equal to 2) is a very convenient approximation to model the atmospheric absorption and scattering of the solar radiation under clear skies. It describes the optical thickness of the atmosphere due to both the absorption by the water vapour and the absorption and scattering by the aerosol particles relative to a dry and clean atmosphere (Kasten 1996; WMO 1981). The larger TL, the larger the attenuation of the radiation by the clear sky atmosphere. It is a convenient parameter to summarize the turbidity of the atmosphere and is often used by engineers and consultants. TL (most usually atmospheric turbidity) is a key input to several models assessing the downwelling irradiance under clear skies that are used several communities in the fields of renewable energies, climatology, agro-meteorology, and atmospheric pollution.

TL can be obtained directly from observations performed during very clear sky periods, but this kind of experimental data is rarely available, thus TL is generally an estimated parameter. Also, time series of radiation data are generally too short to allow estimation on a daily basis. Fortunately, long-term monthly average values, TL_m, are sufficient for most applications. Several methods for estimating TL_m values can be found in the literature: for example from time series of daily global horizontal irradiation (Aguiar, in ESRA 2000); from monthly Angström sum (Page, 1986); from subjective assessments of the type of atmospheric conditions prevailing in the region of interest (linear regression with latitude and with the Atmospheric Turbidity Index, Dogniaux and Lemoine, 1983).

Most often information for specific locations is presented (Jacovides 1997; Pedros *et al.* 1999), though at times, larger areas are dealt with. For example, Gueymard (1994) presents data for several Canadian and Northern USA sites and a Web site supplies values for approximately 600 sites in Europe and vicinity (Angles *et al.* 1998, 1999) derived from the ESRA (2000). The best existing database of surface aerosols is the Aerosol Robotic Network (Aeronet), of which a climatology has been presented by Holben *et al.* (2000) and data can be viewed online (aeronet.gsfc.nasa.gov). The aerosol values can be converted into TL values using existing approximations.

However, TL is mostly unknown worldwide. There is a need for world climatological maps of the Linke turbidity factor (TL) with a cell size of 5' (approx. 10 km at mid-latitude). The availability of such maps will be an important step for the whole community of the stakeholders in solar radiation. No such maps exist presently, even at regional scales.

6 THE METHODOLOGY

Several data sets of the Linke turbidity factor are available. They have been derived from other measurements. They are either values for specific geographical sites or they are under the form of gridded data. The values for specific sites are accurate but have a limited extension in space. The gridded values are covering the whole world. They are given for cells of 280 x 280 km^2 and are space-averaged.

The principle is to fuse these two different sets of information, in order to obtain the final product on a grid with cells of 5' in size. D'Agostino, Zelenka (1992) or Zelenka et al. (1992) proposed solutions to such a problem. In a case similar to ours since they used the same gridded data, Beyer *et al*. (1997) proceed as follows. The original gridded data set is resampled by the means of a bicubic spline and regridded with a regular cell size of 5' x 5' in a canonical projection. It is then assumed that the value in a cell should be equal to the mean of those observed for the measuring stations within the cell. For all cells containing at least a measuring station, the difference between both data sets is computed. Then, these differences are interpolated by the means of a linear unbiased interpolator. The authors abovementioned have employed kriging or co-kriging. The distance for interpolation takes into account the orography. Once the field of the residuals obtained for each cell, this field is added to the gridded data, providing an unbiased gridded map.

The methodology that is used in the construction of the maps of the Linke turbidity factor is derived from that of Beyer *et al*. (1997). The main drawbacks of the previous method lies in the fact that the gridded data that are fused with the sites observations at cells of 5' in size result from an interpolation of the gridded data at cells of 280 km in size. Accordingly, there are no high frequencies in the gridded data at 5', and more exactly, there is no wavenumbers comprised between 5' of arc angle and 150' (approximately 280 km). The gridded data is very smooth. Some high frequencies are locally injected by fusing with sites observations. For areas with no or few observations, the resulting map is still very smooth. The method was appropriate in the case of Beyer *et al*. because a large number of sites observations were available. It is not our case, because large areas are unknown.

Accordingly, we designed a new method. The principle of computing differences for specific sites, interpolating them and finally adding the field of differences to the gridded data is kept. The difference between both methods lies in the construction of approximations of the maps with a cell of 5' before the integration of the sites measurements. In the method of Beyer *et al*., these approximations are resampled gridded data. That means that there is no injection of high frequencies and that the spatial resolution of the gridded data is still 280 km, even if the cell is 5' in size. Only the representation has changed. It follows that we are comparing gridded values and ground measurements that are not comparable because the supports of information are very different. It also follows that the resulting field will be smooth, too. Introduction of the ground measurements will not lead to introduction of high frequencies, except where the network of ground measurements is dense compared to the 2.5 degree distance. In the present method, approximations of the Linke turbidity factor are synthesized at a spatial resolution of 5', which are close to reality, before correcting them by integrating the site measurements. The general solution presented above is used.

It is made of three steps. In the first step, several gridded data having different spatial resolutions and representing different geophysical parameters are fused in order to construct several approximations of the Linke turbidity factor at increasing spatial resolutions. At the end of the first step, the spatial resolution is 20'. In the second step, it is assumed that the value in a cell of 20' in size should be equal to the mean of those observed for the measuring stations within the cell. For all cells containing at least a measuring station, the difference between both data sets is computed. Then, these differences are interpolated by the means of a linear unbiased interpolator. Once the field of the residuals obtained for each cell, this field is added to the gridded data, providing an unbiased gridded map. In the last step, the final products are constructed by fusing the gridded data at 20' with orography, using a similar approach than in the first step.

In principle, a two-steps approach would suffice. The fusion of sites observations and gridded data can be made at the cell of 5' in size, instead of 20' and the third step is not necessary. However, the size of the data to handle at a 5' resolution is large: the matrix of values is 4320 times 2160 pixels. Running an interpolation process based on a distance weighted by the difference in latitudes and in orography, and calling upon approximately 250 sites observations, request a large amount of computational resources. These resources are beyond the capabilities of Meteotest in the framework of this project. Accordingly, a trade-off was found. The fusion of sites observations and gridded data is performed with a cell of 20' in size and the third step permits to obtain the final product at 5' by a fusion of additional gridded data.

7 THE GRIDDED DATA

Gridded data are available that report monthly clear sky irradiations (Staylor approximation). They are supplied by the NASA-Langley Research Center, in the framework of the Solar Radiation Budget Project SRB (DiPasquale & Whitlock 1992; Whitlock

1995). From these data, the TL can be computed (Remund *et al.* 2003) by an iterative application of the ESRA clear-sky model (Rigollier *et al.* 2000) with modifications (Geiger *et al.* 2002).

The cell is an equal area cell everywhere of 280 x 280 km². At mid-latitude, it corresponds to approximately 2.5 x 2.5 degrees² of arc angle. The twelve maps (one per month) of TL were re-mapped using the canonical projection. This is performed by the means of the spline bi-cubic operator. A mirror technique is used for the edges. The cells are squared and have a size of 160' of arc angle. This initial set of maps is called the set TL_{SRB} (Fig. 1).

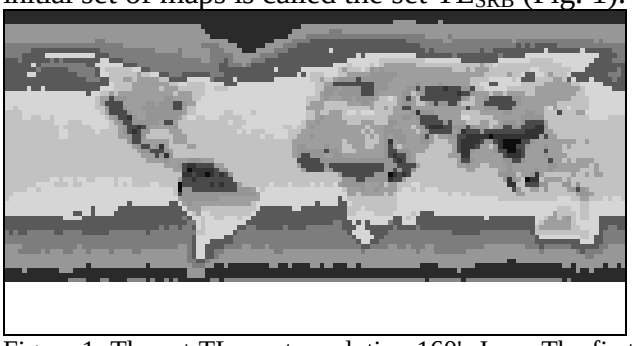

Figure 1. The set TL_{SRB} at resolution 160'. June. The first line is latitude 90 N, the last is 90 S. The first column is longitude 180 W, the last is 180 E. Black: large value (approx. 6); white: low value (approx. 1, or unknown for the Antarctic part).

The atmospheric turbidity is a function of the amount of water vapour in the atmosphere. Within the NVAP (NASA Water Vapor Project), the NASA Langley Research Center Atmospheric Sciences Data Center combined several observations to construct world-wide maps of the content of water vapour integrated over the total column (Randel *et al.* 1996). The gridded data are available on the Internet (NVAP 2001). The monthly mean value for each cell over the 10 years (1988-97) is computed (Fig. 2).

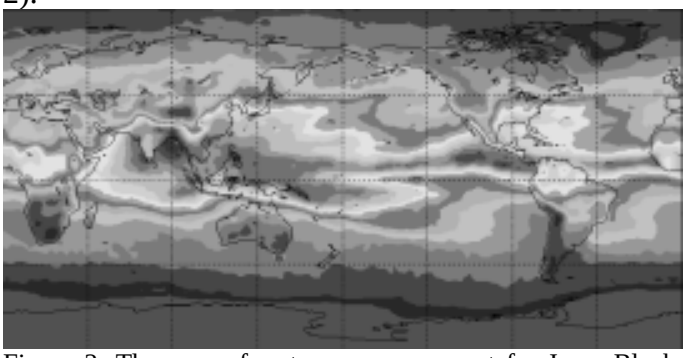

Figure 2. The map of water vapour amount for June. Black: low value; white: large value.

The NVAP maps are re-mapped as above. The cells are squared and have a size of 80' of arc angle. The relation between TL_{SRB} and NVAP (in mm) was assessed over land at resolution 160' by linear regression (Table 1):

$$TL_{SRB} = a \ln NVAP + b \quad (8)$$

Table 1. Parameters of Eq. 8

	a	*b*		*a*	*b*
Jan	30.7235	-33.3767	Jul	35.4256	-45.4808
Feb	31.312	-32.0650	Aug	-14.3931	152.9660
Mar	26.8757	-13.3799	Sep	5.0209	78.3512
Apr	14.8917	35.4049	Oct	13.9920	37.5755
May	3.3993	82.0606	Nov	25.1935	-10.5575
Jun	31.7095	-32.5927	Dec	33.1209	-42.3625

This data set NVAP is used for resolutions comprised between 80' and 160' over land.

The third data set TL_{TMAP} is composed of maps of the TL, over the oceans only. They are computed from the maps of aerosol optical depth at 630 µm for several years (1985-99) found on the Web server of the Thermal Modeling and Analysis Project (TMAP) at NOAA Pacific Marine Environmental Laboratory (TMAP 2001). The twelve maps were re-mapped as above. The cells are squared and have a size of 80' of arc angle. This data set is used for resolutions 80' to 160' over the oceans.

The fourth data set is a worldwide digital terrain model with a cell size of 5' (TerrainBase 1995). This data set is used from resolution 5' to 80'.

By application of the general solution described above, one obtains twelve maps of the parameter TL with a cell size of 5'. Here, we used the MSM of Starck & Murtagh (1994).

8 MERGING GRIDDED DATA AND GROUND MEASUREMENTS

These gridded data are subsampled down to 20' before merging with ground data. The TL of the stations are corrected to the altitude of the cell. For all cells containing at least a measuring station, the difference between both data sets is computed. Then, these differences are interpolated by the means of a linear unbiased interpolator using the inverse of the squared distance. The distance is that of Lefèvre *et al.* (2002) which is based on the geodetic distance and takes into account the latitudinal anisotropy of the meteorological phenomena and the difference in elevation.

Once the field of the residuals obtained for each cell, this field is added to the gridded data, providing an unbiased gridded map which is resampled up to 5'. This final map is presented in Fig. 3 for the month of June.

One may note that both maps (Figs. 1 and 3) are similar for large scales. The second one exhibits high frequencies, which are those found in the external data. A close examination reveals some artefacts that originate from the TMAP or NVAP data. The maps look spotty, but most of the spots can be explained. Several regional effects like wood burning are not included in the background map but in the ground information. Because of the low density of ground stations (outside Europe and North America) some of the local effects are mapped as spots. Many tropical stations show high aerosol values just before

rainy season, when the wood is burned (see September/October in the Amazon region). The Sahel zone exhibits high turbidity values during the whole year.

These maps for the twelve months are available on line at the web site (www.soda-is.com) of the SoDa service delivering information on the solar radiation at ground level (Wald *et al.* 2002).

9 QUALITY OF THE ASSESSMENT

The quality of the retrieval is assessed by performing the above-described operations with all the stations but one. By iteration and changing the removed station at each iteration, one gets a series of discrepancies between the observed TL and the estimates. From this series are computed the bias (MBE) and the root mean square error (RMSE) and reported in Table 2. This is called the effective error. The RMSE is influenced by outliers in the tropics where the distances between sites are very large and the values vary very much in space. About 6 out of 220 sites were eliminated for calculating the effective error.

In order to evaluate the benefit of the fusion with ground measurements, a second test was made and characterises the error for the first step of the procedure, *i.e.* constructing a gridded map at 20' resolution. The cell values are then compared to ground measurements (columns "first step" in Table 2). Remembering that the TL varies approximately between 1 and 6, the MBE after the first step is quite high as well as the RMSE.

The fusion with ground measurements is very beneficial. The bias is null. The RMSE error lies between 0.6 (Dec.) and 0.9 (March) with an average value of 0.7.

Table 2. Assessment of the quality

Month	Number of sites	First step		Effective error	
		MBE	RMSE	MBE	RMSE
January	222	-0.6	1.2	0.0	0.7
February	230	-0.7	1.3	0.0	0.7
March	228	-0.6	1.2	-0.1	0.9
April	230	-0.4	1.1	0.0	0.7
May	239	-0.2	1.1	0.0	0.7
June	240	-0.1	1.0	0.0	0.8
July	238	0.0	1.0	0.0	0.8
August	239	-0.2	1.0	0.0	0.8
September	238	-0.4	1.1	0.0	0.7
October	229	-0.3	1.0	0.0	0.7
November	227	-0.4	1.0	0.0	0.7
December	219	-0.5	0.9	0.1	0.6
Mean		-0.4	1.1	0.0	0.7

10 CONCLUSION

The ARSIS concept has mostly been used with images at high or very high spatial resolution. The present study demonstrates its potentials in climatology. By the means of a fusion process, it has been possible to synthesize climatological maps of the atmospheric turbidity at a much finer resolution than the initial one.

The standard implementations of the ARSIS concept, and especially the Inter-Modality Models (IMM), apply to the high frequencies (Ranchin & Wald 2000). Here, the IMM is assessed on the approximations themselves; the HRIMM (High Resolution IMM) is applied on the high frequencies.

Another innovation in this implementation is its iterative process: at each resolution, two syntheses are performed. They are separated by an analysis process and a substitution of the analysis results by the fused product obtained at the previous resolution. In current implementations, the HRIMM replicates the model IMM and comprises only one synthesis. This approach was selected here to ensure that i) the fused product is equal to the initial one once resampled to the initial resolution and ii) the intensity of injected high frequencies is reasonable in order to avoid spatial artefacts.

Owing to this fusion method, twelve climatological maps of the Linke turbidity factor were constructed, one per month. Their availability and their quality are an important step for the whole community of the stakeholders in solar radiation. The quality was estimated as offering a RMSE of 0.7. This may be considered as of low quality. It should be stressed that, even in this case, the construction of such maps is a significant step forward the state-of-the-art and that nobody can provide values of the Linke turbidity factor with a much greater accuracy, except at the relatively rare sites where specific observations are made.

ACKNOWLEDGEMENTS

This work was supported by the European Commission (DG-INFSO) under Contract Number IST-1999-12245 (project SoDa). Many thanks goes to H. Gilgen and A. Ohmura of Institute for Atmosphere and Climate ETH (IACETH) for BSRN data and data of Payerne and Reckenholz. Further we thank the principal investigators Brent Holben and Chuck McClain from GSFC, NASA and Didier Tanré from Univ. Lille for Aeronet level 2.0 data. The Australian Regional Instrument Center, Bureau of Meteorology provided a CD-ROM with global and beam irradiance data of several years. Swiss Meteorological Institute (SMI) provided data of ten stations and the Swiss Agency for Environment, Forest and Landscape (SAEFL) data of five NABEL stations.

REFERENCES

Aiazzi, B., Alparone, L., Argenti, F. & Baronti, S., 1999. Wavelet and pyramid techniques for multisensor data fusion: a performance comparison varying with scale ratios. In *Image and Signal Processing for Remote Sensing V*, S. B. Serpico, Ed., SPIE vol. 3871: 251-262.

Angles, J., Menard, L., Bauer, O. & Wald, L., 1998. A Web server for accessing a database on solar radiation parameters. In *Proceedings of the Earth Observation & Geo-Spatial Web and Internet Workshop '98*, Josef Strobl & Clive Best Eds, Salzburger Geographische Materialien, Universität Salzburg, Salzburg, Austria, Heft 27, pp. 33-34.

Angles, J., Menard, L., Bauer, O., Rigollier, C. & Wald L., 1999. A climatological database of the Linke turbidity factor. In *Proceedings of the ISES Solar World Congress 1999*, Jerusalem, Israel, July 4-9, 1999, volume I, pp 432-434.

Beyer, H.-G., Czeplak, G., Terzenbach, U. & Wald, L., 1997. Assessment of the method used to construct clearness index maps for the new European solar radiation atlas (ESRA). *Solar Energy*, Vol. 61 (No. 6): 389-397.

D'Agostino, V. & Zelenka, A., 1992. Estimating solar global irradiance by integration of satellite and network data: the cokriging approach. *Sciences de la Terre, Sér. Inf.*, Vol. 31: 461-465.

DiPasquale, R.C. & Whitlock, C.H., 1992. Global distribution of shortwave fluxes derived from satellite data for the world climate research programme, *International Journal of Climatology*, Vol. 15: 961-974.

Dogniaux, R. & Lemoine, M., 1983. In: W. Palz (Ed.), Solar Energy R&D in the European Community, Series F, Vol. 2, *Solar Radiation Data*. D. Reidel Publ., Dordrecht, pp. 94-107.

Dutilleux, P., 1989. An implementation of the "algorithme à trous" to compute the wavelet transform. In: Combes, J. M., Grossman, A., Tchamitchian, Ph. (Eds.), *Wavelets: Time-Frequency Methods and Phase Space*. Springer, Berlin, pp. 298-304.

ESRA *European Solar Radiation Atlas*, 2000, includ. CD-ROM. Edited by J. Greif, K. Scharmer. Scientific advisors: R. Dogniaux, J. K. Page. Authors : L. Wald, M. Albuisson, G. Czeplak, B. Bourges, R. Aguiar, H. Lund, A. Joukoff, U. Terzenbach, H. G. Beyer, E. P. Borisenko. Published for the Commission of the European Communities by Les Presses de l'Ecole des Mines de Paris, France.

Geiger, M., Diabaté, L., Ménard, L. & Wald, L., 2002. A web service for controlling the quality of measurements of global solar irradiation. *Solar Energy*, Vol. 73 (No 6): 475-480.

Gueymard, C., 1994. Analysis of monthly average atmospheric precipitable water and turbidity in Canada and Northern United States. *Solar Energy*, Vol. 53 (No 1): 57-71.

Holben, B.N., Tanré, D., Smirnov, A., Eck, T.F., Slutsker, I., Abuhassan, N., Newcomb, W.W., Schafer, J.S., Chatenet, B., Lavenue, F., Kaufman, Y.J., Van de Castle, J., Setzer, A., Markham, B., Clark, D., Frouin, R., Halethore, R., Karnieli, A., O'Neill, N.T., Pietras, C., Pinker, R.T., Voss, K. & Zibordi, G., 2001. An emerging ground-based aerosol climatology. Aerosol optical depth from Aeronet. *Journal of Geophysical Research*, 106D: 12067-12097.

Jacovides, C.P., 1997. Model comparison for the calculation of Linke turbidity factor. *International Journal of Climatology*, Vol. 17: 551-563.

Kasten, F., 1996. The Linke turbidity factor based on improved values of the integral Rayleigh optical thickness. *Solar Energy*, Vol. 56: 239-244.

Lefèvre, M., Remund, J., Albuisson, M. & Wald, L., 2002. Study of effective distances for interpolation schemes in meteorology. European Geophysical Society, 27th General Assembly, *Geophysical Research Abstracts*, vol. 4, EGS02-A-03429.

Mallat, S. G., 1989. A theory for multiresolution signal decomposition: the wavelet representation. *IEEE Transactions on Pattern Analysis and Machine Intelligence*, Vol. 11 (No. 7): 674-693.

NVAP 2001. NASA Water Vapor Project. NASA Langley Research Center Atmospheric Sciences Data Center, Web site: http://eosweb.larc.nasa.gov, as of 2001.

Page, J.K., Ed., 1986. *Prediction of solar radiation on inclined surfaces*. Solar Energy R&D in the European Community, Series F, Vol. 3, Solar Radiation Data, D. Reidel Publishing Compagny, Dordrecht, Holland.

Pedros, R., Utrillas, J.A., Martinez-Lozano, J.A. & Tena, F., 1999. Values of broad band turbidity coefficients in a mediterranean coastal site. *Solar Energy*, Vol. 66 (No 1): 11-20.

Ranchin, T., Aiazzi, B., Alparone, L., Baronti, S. & Wald, L. 2003. Fusion of images for urban areas studies. The ARSIS concept and some successful implementation schemes. *ISPRS Journal of Photogrammetry & Remote Sensing*, Vol. 58: 4-18.

Ranchin, T. & Wald, L., 2000. Fusion of high spatial and spectral resolution images: the ARSIS concept and its implementation. *Photogrammetric Engineering and Remote Sensing*, Vol. 66 (No 1): 49-61.

Randel, D.L., Vonder Haar, T.H., Ringerud, M.A., Stephens, G.L., Greenwald, T.J. & Combs, C.L., 1996. A new global water vapor dataset. *Bulletin of the American Meteorological Society*, Vol. 77 (No 6).

Remund, J., Wald, L., Lefèvre, M., Ranchin, T. & Page, J., 2003. Worldwide Linke turbidity information, To be presented at ISES 2003 (International Solar Energy Society), Goeteborg, Sweden, 16-19 June 2003.

Rigollier, C., Bauer, O. & Wald, L., 2000. On the clear sky model of the 4th European Solar Radiation Atlas with respect to the Heliosat method. *Solar Energy*, Vol. 68 (No 1): 33-48.

Starck, J.-L. & Murtagh, F., 1994. Image restoration with noise suppression using the wavelet transform. *Astronomy Astrophysics*, Vol. 288: 342-350.

TerrainBase 1995. *TerrainBase: Worldwide Digital Terrain Data*. Documentation Manual, CD-ROM Release 1.0, NOAA, National Geophysical Data Center, Boulder, Colorado, USA, April 1995.

TMAP 2001. Thermal Modeling and Analysis Project. NOAA Pacific Marine Environmental Laboratory, http://las.saa.noaa.gov/las-bin/climate_server/dset= AVHRR+PATHFINDER, as for August 2001.

Wald, L., 2002. *Data Fusion. Definitions and Architectures - Fusion of Images of Different Spatial Resolutions,* Les Presses de l'Ecole des Mines de Paris, Paris, France.

Wald, L., Albuisson, M., Best, C., Delamare, C., Dumortier, D., Gaboardi, E., Hammer, A., Heinemann, D., Kift, R., Kunz, S., Lefèvre, M., Leroy, S., Martinoli, M., Ménard, L., Page, J., Prager, T., Ratto, C., Reise, C., Remund, J., Rimoczi-Paal, A., Van der Goot, E., Vanroy, F. & Webb, A., 2002. SoDa: a project for the integration and exploitation of networked solar radiation databases. In: *Environmental Communication in the Information Society*, W. Pillmann, K. Tochtermann Eds, Part 2, pp. 713-720. Published by the International Society for Environmental Protection, Vienna, Austria.

Whitlock, C.H., 1995. First global WCRP shortwave surface radiation budget dataset. *Bulletin of the American Meteorological Society*, Vol. 76: 905-922.

WMO (World Meteorological Organization) 1981. *Technical Note No. 172, WMO-No. 557*, Geneva, Switzerland, pp. 121-123.

Zelenka, A., Czeplak, G., d'Agostino, V., Josefson, W., Maxwell, E. & Perez, R., 1992. *Techniques for supplementing solar radiation network data, Technical Report* (3 volumes), International Energy Agency, # IEA-SHCP-9D-1, Swiss Meteorological Institute, Krahbuhlstrasse, 58, CH-8044 Zurich, Switzerland.

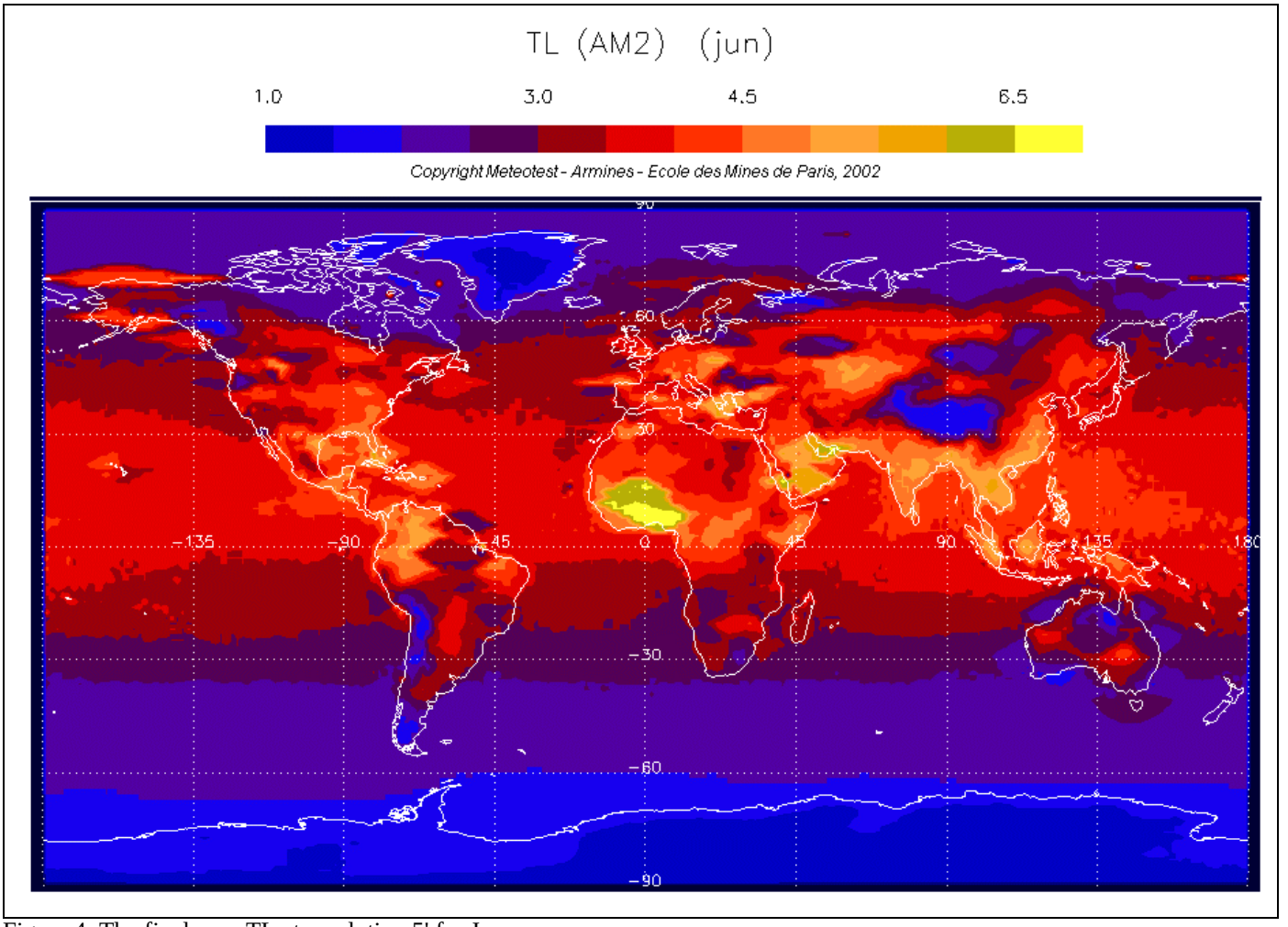

Figure 4. The final map TL at resolution 5' for June.